

RESEARCH

Open Access

GEMs and amplitude bounds in the colored Boulatov model

Francesco Caravelli

Abstract

In this paper, we construct a methodology for separating divergencies due to different topological manifolds dual to Feynman graphs in a colored group field theory. After having introduced the amplitude bounds using propagator cuts, we show how Graph-Encoded Manifold (GEM) techniques can be used in order to factorize divergencies related to different parts of the dual topologies of the Feynman graphs in the general case. We show the potential of the formalism in the case of three-dimensional solid torii in the colored Boulatov model.

Keywords: GFT; GEMs; Topology; Large N ; Quantum gravity

Introduction

Recently, there has been a growth of interest in group field theories [1-3], and there are many reasons for this to happen, first of all because these are connected with spin foams [4]. Spin foams are a formalization of covariant time evolution in Loop Quantum Gravity, and group field theories can be seen as a formalization of their partition function expansion. In this sense, group field theories (GFTs) can be formalized as a quantum field theory over a group manifold and are a generalization of matrix models to higher dimensions [5,6]. It is known that matrix models have a topological expansion in which the genus, the only topological invariant needed to characterize two surfaces, plays the role of a parameter of this expansion.

Roughly speaking, an n -dimensional GFT has a vertex associated to an n -simplex and a propagator which glues the n -simplices along their $(n - 1)$ -dimensional boundary faces. The Feynman diagrams of an n -dimensional GFT, in their dual, can be interpreted as gluings of simplices and then have the interpretation of piecewise linear (PL) manifolds. However, generic GFTs in three dimensions have the problem that the gluings are too arbitrary, in the sense that the generated simplicial complexes are not even pseudo-manifolds since they present wrapping singularities [7]. As in an ordinary ϕ^4 theory, a three-dimensional GFT can generate an '8' diagram of which the dual has no obvious topological interpretation in the continuum limit.

This phenomenon does not happen in two dimensions, and the hope is that these singularities can be removed in the continuum limit. For this reason, a *colored* version of group field theory (cGFT) was introduced in an arbitrary number of dimensions (see [2,8] and references therein), not to mention a generalization of group field theory to tensor [9], for which a universality theorem has been proven in the case of independent fluctuations [10]. The challenge in these models is to obtain a topological expansion as in the two-dimensional case [11-15]. It has been shown in [16], and in an arbitrary number of dimensions, that diagrams whose dual topology is a sphere dominates the partition function in the limit of the cutoff being removed. In order to achieve this result, techniques from the theory of crystallizations [17,18] have been used. Colored n -graphs are well known in mathematics as graph-encoded manifolds (GEMs) [17,18]. In a previous paper [19], we used GEM techniques in order to prove the orientability of pseudo-manifolds generated in a cGFT in any dimensions, based on the fact that these generate only bipartite graphs. In this paper, we base our methodology on another theorem proven in the field of crystallizations, which puts in relation dipole contractions and the connected sum of manifolds.

In order to further clarify the background, we briefly give a review of the context. There is a class of graphs which plays a special role in cGFT. These are called melonic graphs. The simpler of these is a two-node graph in which all but two of the propagators are connected,

Correspondence: f.caravelli@ucl.ac.uk
QASER Lab, University College London, Gower Street, London WC1E 6BT, UK

which are of the same color. Now, we can construct any type of melonic graph from this by inserting a melonic graph inside each of the propagators in all possible combinations. It is easy to see that this type of graphs can be classified in terms of trees. It has been shown in [16] that this class of graphs, remarkably, dominate the partition function in the limit in which the cutoff goes to infinity, and in particular, their duals are always associated to spheres. In fact, within each perturbative order, melonic graphs have the highest divergence. Initiated by [16], a series of studies [20-24] has elucidated the structure of the divergencies in many cases, and a class of renormalizable theories have been introduced in [25,26]. However, as noted in [27] and further studied in [28], spheres are combinatorially not favored for other topologies in the perturbative expansion. For this reason, we believe it is important to have an understanding of the corrections to the path integral given by Feynman graphs whose duals correspond to topologies other than spheres, and techniques like those we will introduce in the body of this paper could be potentially useful.

We will try to address this in a framework of ‘topological’ cuts. How do we separate the divergencies coming from spheres and those coming from other topologies? In other terms, how do we factorize these divergencies? A step towards this type of problem will be put forward in this paper, where we will argue that performing the cuts strategically factorizes graphs whose duals are spheres. When these cuts are performed, the graphs combine into connected sums, and thus, the remaining graphs is actually a well-defined surgery operation in topology.

For the case of a 3-manifold, a theorem [29] ensures that that every compact and orientable 3-manifold can be decomposed uniquely into the connected sum of prime manifolds. Although a group field theory generates only pseudo-manifolds, their orientability has been shown in [19]. Thus, if we were able to eliminate pseudo-manifolds from the partition function, the techniques developed in this paper could be very useful. In the following, we will focus on a three-dimensional cGFT, in particular the colored Boulatov model, as the theorem we will make use of is based on a three-dimensional topology.

The paper is organized as follows: in the section ‘The colored Boulatov model and 3-GEMs,’ we recall the colored Boulatov model and its standard interpretation. In the section ‘Topological bounds from cuts,’ we develop the cut strategy and the main result of this paper, and in the section ‘Solid torus decomposition,’ we apply it to the connected sum of solid torii as an example. Conclusions follow.

The colored Boulatov model and 3-GEMs

We now introduce the colored Boulatov model [8,30]. Consider a compact Lie group G , denote h its elements,

e the unit element, and $\int dh$ the integral with respect to the Haar measure of the group.

In three dimensions, we introduce two fields, $\bar{\psi}^i$ and ψ^i , and let $i = 0, 1, 2, 3$ be four couples of complex scalar (or Grassmann) fields over four copies of G , $\psi^i : G \times G \times G \times G \rightarrow \mathbb{C}$.

In a generic number of dimensions, $i = 0, \dots, n + 1$ where n is the number of dimensions, and the ψ and $\bar{\psi}$ are functions of n copies of the group. We define e as the identity element of the group, and we denote $\delta^\Lambda(h)$ as the regularized delta function over G with some cutoff Λ such that $\delta^\Lambda(e)$ is finite but diverges when Λ goes to infinity. A feasible regularization is given, for instance for the group $G = SU(2)$, by

$$\delta^\Lambda(h) = \sum_{j=0}^{\Lambda} (2j + 1) \chi^j(h) \tag{1}$$

where $\chi^j(h)$ is the character of h in the representation j and preserves the composition properties. The path integral for the colored Boulatov model over G is

$$Z(\lambda, \bar{\lambda}) = e^{-F(\lambda, \bar{\lambda})} = \int \prod_{i=0}^3 d\mu_P(\bar{\psi}^i, \psi^i) e^{-S^{\text{int}}(\bar{\psi}^i, \psi^i)}, \tag{2}$$

where the Gaussian measure $d\mu_P$, with P being its covariance, is chosen such that

$$\int \prod_{i=0}^4 d\mu_P(\bar{\psi}^i, \psi^i) = 1,$$

and

$$\begin{aligned} P_{h_0 h_1 h_2; h'_0 h'_1 h'_2} &= \int d\mu_P(\bar{\psi}^i, \psi^i) \bar{\psi}_{h_0 h_1 h_2}^i \psi_{h'_0 h'_1 h'_2}^i = \\ &= \int dh \delta^\Lambda(h_0 h(h'_0)^{-1}) \delta^\Lambda(h_1 h(h'_1)^{-1}) \\ &\quad \times \delta^\Lambda(h_2 h(h'_2)^{-1}). \end{aligned}$$

The colored model has two interactions, a ‘clockwise’ and an ‘anticlockwise,’ and one is obtained from the other one by complex conjugation in the internal group color, one for each face of the 3-simplex. We fix the notation for shortage of space, $\psi(h, p, q) = \psi_{h p q}$. There are two interaction terms:

$$\begin{aligned} S^{\text{int}} &= \frac{\lambda}{\sqrt{\delta^\Lambda(e)}} \int \prod_{i,j} dh_{i,j} \psi_{h_{03} h_{02} h_{01}}^0 \psi_{h_{10} h_{13} h_{12}}^1 \psi_{h_{21} h_{20} h_{23}}^2 \psi_{h_{32} h_{31} h_{30}}^3 \\ &\quad + \frac{\bar{\lambda}}{\sqrt{\delta^\Lambda(e)}} \int \prod_{i,j} dh_{i,j} \bar{\psi}_{h_{03} h_{02} h_{01}}^0 \bar{\psi}_{h_{10} h_{13} h_{12}}^1 \bar{\psi}_{h_{21} h_{20} h_{23}}^2 \bar{\psi}_{h_{32} h_{31} h_{30}}^3 \end{aligned} \tag{3}$$

where $h_{ij} = h_{ji}$. In order to make the notation clearer, we call ‘red’ the vertex involving the ψ ’s and ‘black’ the one involving the $\bar{\psi}$ ’s (Figure 1). Thus, any line coming out of

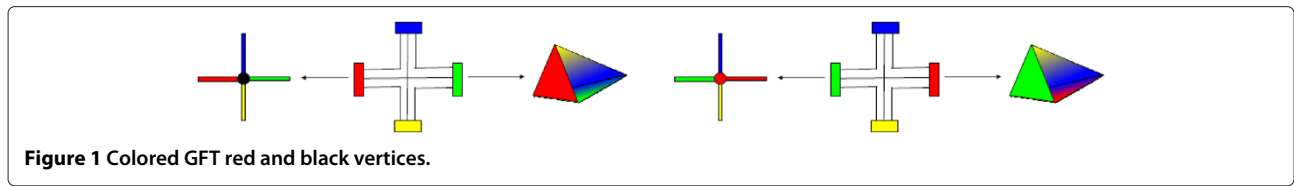


Figure 1 Colored GFT red and black vertices.

a cGFT vertex has a color i . The group elements h_{ij} in Equation 3 are associated to a field and glue two vertices with opposite orientation.

In the body of this paper, we will consider only vacuum graphs, i.e., all the vertices of all the graphs are 4-valent (no open lines) and we will only deal with connected graphs. The strands of a vacuum cGFT graph Γ have a natural orientation given by the fact that only vertices of opposite orientations can be glued. It is easy to see that a vacuum cGFT graph must have the same number of black and red vertices. For any graph Γ , consider the set \mathcal{V}_Γ of its vertices, $|\mathcal{V}_\Gamma| = 2n$, and the set \mathcal{L}_Γ as its edges; and we define as *faces* \mathcal{F}_Γ (not to be confused with the faces of the tetrahedron!) as any closed line in the Feynman graph of a GFT.

A generic vacuum Feynman amplitude of the theory can be written as

$$\mathcal{A} = \frac{(\lambda\bar{\lambda})^{\frac{n}{2}}}{[\delta^\Lambda(e)]^n} \int \prod_{l \in \mathcal{L}_\Gamma} dh_l \prod_{f \in \mathcal{F}_\Gamma} \delta_f^\Lambda \left(\prod_{l_0 \in f} h_{l_0}^{\sigma_{l_0|f}} \right), \quad (4)$$

where the notation $l_0 \in f$ means that the line l belongs to the face f and $\sigma_{l_0|f} = 1$ (respectively -1) if the orientations of l and f coincide (are respectively opposite). In the following, we will assume that an orientation is fixed. The δ^Λ functions are invariant under cyclic permutations and conjugation of their arguments. Hence, the amplitude of a graph does not depend on the orientation of the faces.

We now recall few facts about three graph-embedded pseudo-manifolds, which are strictly related to the colored Boulatov model and enlight the topological properties of the Feynman graph duals. Let Γ be a finite, edge-colored graph. A k -bubble in the spinfoam literature of Γ , $k \in \mathbf{N}$ is a connected component of subgraph of Γ induced by k colors.

These graphs represent a piecewise linear pseudo-complex in the following sense [31]. Let Γ be a 4-regular graph and γ its coloring. To a couple $(\Gamma, \gamma)_{n+1}$, there is an associated *pseudo-complex* $K(\Gamma)$ given by the following construction. Take an n -simplex σ^n for each \mathcal{V}_Γ and label its vertices Δ_n . If x_i, y_j in \mathcal{V}_Γ are joined by an edge, then we glue also the related $(n - 1)$ -simplices. In the case of a tetrahedron, this means gluing the faces of the tetrahedron, which are triangles, of the same color. We denote with $|\Gamma|$ the pseudo-complex associated with the colored graph Γ . It is the color that makes this pro-

cedure unambiguous as there is only one color for each face of the tetrahedron. This is the same interpretation given to connecting vertices (of opposite orientation) in a (colored) n -dimensional GFT. This is also the reason why colored group field theories have a clear interpretation as orientable pseudo-manifolds [19]. Thus, given the above description of a pseudo-complex, cGFTs are associated to complexes in the following sense: a vertex can be seen as the dual of a tetrahedron and, its propagators represent gluings of the triangles which form the tetrahedron of the same color.

Each propagator is actually decomposed into three *parallel* strands which are associated to the three arguments (group elements) of the fields, i.e., the one-dimensional elements of the 1-skeleton of the tetrahedron which bound every face. A line represents the gluing of two tetrahedra (of opposite orientations) along triangles of the same color as in Figure 2.

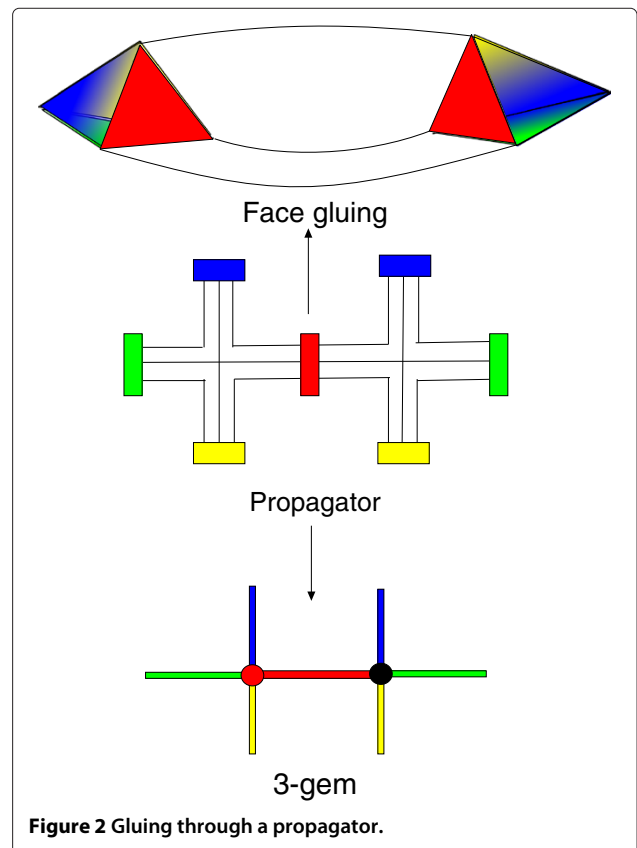


Figure 2 Gluing through a propagator.

Another operation which we need to introduce is the connected sum of two manifolds, denoted by the symbol $\#$. The connected sum of the two manifolds M_1 and M_2 is given by $M \cong M_1 \# M_2$. If both manifolds are oriented, there is a unique connected sum operation. Consider two balls, one in M_1 and one in M_2 . Carve the two balls and glue their boundaries with opposite orientation. The points where the two balls have been carved denotes the two points which characterize the operation, which is then $\#_{p_1,p_2}$. The result is unique up to homeomorphisms, and thus when the base points will be omitted, the result will not be ambiguous.

We now introduce dipole contractions and creations. Dipole contraction is an operation performed between two nodes of a Feynman colored graph, as described in Figure 3 for the case of a 4-colored graph.

We call two dipoles degenerate if they belong to the same bubble and nondegenerate otherwise. We now introduce the main theorem which will be central to our analysis hereafter [18].

Theorem 1. (Dipole contraction) *Let u and v be vertices in a 4-graph connected by an m -dipole, and Γ_1 and Γ_2 be two colored 4-graphs. If S^n is the n -dimensional sphere, we have*

- a. $|\Gamma_1 \#_{uv} \Gamma_2| \cong |\Gamma_1| \# |\Gamma_2|$
- b. *If u and v are not contained in the same 3-bubble of Γ_1 and Γ_2 is obtained from Γ_1 by fusion on u and v , then $|\Gamma_2| \cong |\Gamma_1| \# S^1 \otimes S^2$*
- c. *If Γ_1 is obtained from Γ_2 by removing a degenerate 2-dipole, then $|\Gamma_2| \cong |\Gamma_1| \# S^1 \otimes S^2$*
- d. *If Γ_1 is obtained from Γ_2 by removing a degenerate 1-dipole, then one of the following cases hold:*
 - (i) $|\Gamma_1| \cong |\Gamma_2|$ *if u and v are contained in a 2-bubble*
 - (ii) $|\Gamma_1| \cong |\Gamma_2| \# S^1 \otimes S^2$ *if u and v are contained in two different 2-bubbles*
 - (iii) $|\Gamma_1| \cong |\Gamma_2| \# S^1 \otimes S^2 \# S^1 \otimes S^2$ *if three such 2-bubbles and Γ_2 are connected*

- (iv) $|\Gamma_1| \cong |\Gamma'_1| \# |\Gamma'_2| \# S^1 \otimes S^2$ *if three such 2-bubbles and Γ_2 has two connected components Γ'_1 and Γ'_2*

depending on whether the endpoints u and v of the dipole are both contained on exactly (i) one 2-bubble with colors other than that of edge $\{u,v\}$, (ii) two such 2-bubbles, (iii) three such 2-bubbles and Γ' that is connected, or (iv) three such 2-bubbles and Γ' that has two connected components Γ'_1 and Γ'_2 . This theorem is fundamental in order to have a clear understanding of the topology associated with graphs generated by a cGFT, and it will be extensively used in the rest of the paper as it also makes clear the role of the connected sum operation in relation to dipole moves.

Let us first make some remarks. The first thing we note is that the connected sum of the spheres is given by only 2- and 3-dipoles. Thus, by a subsequent contraction of these, we can always return to a graph with two nodes, and according to the theorem above, this will be homeomorphic to the sphere. This is true, for instance, for the graphs in Figure 4. As we will see later, however, the divergencies of the two graphs shown in Figure 4 are different. These are two examplicative cases. The reason is that 2-dipoles in 'parallel' generate divergencies, while 2-dipoles in series do not. This is the reason why 2-dipoles are quite bad to handle, while 3-dipoles are not (they always produce a divergence and contract to a line). Moreover, this is the main difference between two-dimensional matrix models and their generalizations in higher dimensions. In the case of two-dimensional matrix models, adding a sphere does not produce any divergence because of the 3-dipoles. The reason is that $S_2 \# S_2$ still has the same genus and thus, in the 't Hooft, limit the scale in the same fashion. The three-dimensional case is, as we have just remarked, quite different. We would like to make the point that genus zero manifolds in three dimensions are *unique*: adding or not a sphere does not change the topology at all. Moreover, amplitudes are independent under the change of orientation of the manifold as this is the same as acting through the color symmetry of the group field theory [19].

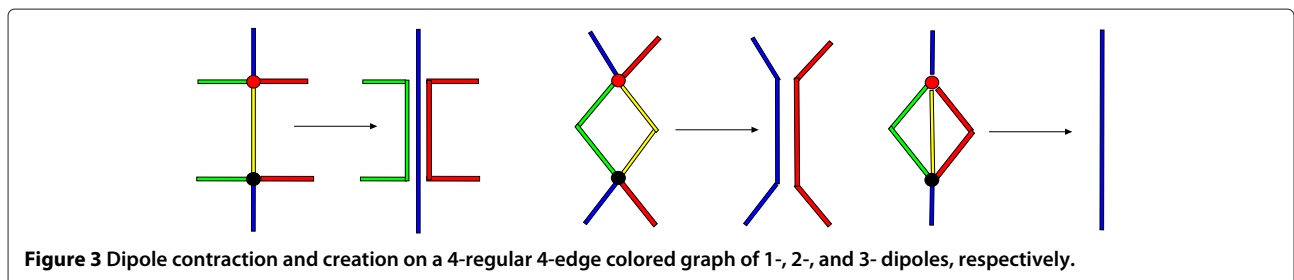


Figure 3 Dipole contraction and creation on a 4-regular 4-edge colored graph of 1-, 2-, and 3- dipoles, respectively.

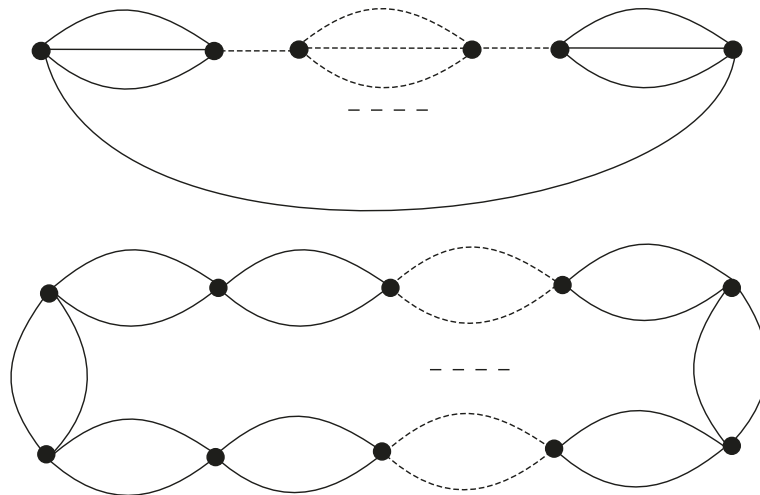


Figure 4 Connected sum of spheres S^3 . The graph on top has a divergence degree proportional to the number of vertices, while the graph at the bottom has a divergence degree independent from the number of vertices.

The first connected sum we construct is that of the sphere, shown in the graph in Figure 4, which is

$$S^3 \simeq [S^3]^n = \underbrace{S^3 \# S^3 \# \dots \# S^3}_{n\text{-times}} \quad (5)$$

and the amplitude associated with the graph is

$$\mathcal{A}_{2n}(S^3) \sim \lambda^n \bar{\lambda}^n [\delta^\Lambda(e)]^{n+2}. \quad (6)$$

This is topologically an identity, but from the point of view of divergencies, it is not. This can be seen from the two graphs in Figure 4. Evaluating these amplitudes is an exercise, and they can be evaluated using the rules in Figures 5 and 6.

Definition 1. A 4-edge-colored 4-graph is said to be *minimal* for the topological 3-manifold \mathcal{M} if it is a 3-GEM representation of \mathcal{M} with the minimal number of vertices. For instance, the minimal graph for the sphere is made of

two vertices, while the minimal graph for the solid 3-torus is in Figure 7.

Topological bounds from cuts

Sphere amplitudes

As it has been shown recently [16], 3-spheres play a special role in three-dimensional group field theories, a role played indeed by 2-spheres in matrix models. It is true that 3-balls (in the case of vacuum graphs) dominate the partition function of cGFT in the limit in which the cutoff Λ goes to infinity, but if we do not keep the cutoff finite, other topologies contribute to the partition function. The result, *a posteriori*, is not surprising for the following argument. For a generic 4-colored graph G of $2n$ -vertices in a D -dimensional GFT, the following bound holds on its associated amplitude [32]:

$$\mathcal{A}(G) \leq K^{2n} \Lambda^{3(D-1)(D-2)n/2+3(D-1)} \quad (7)$$

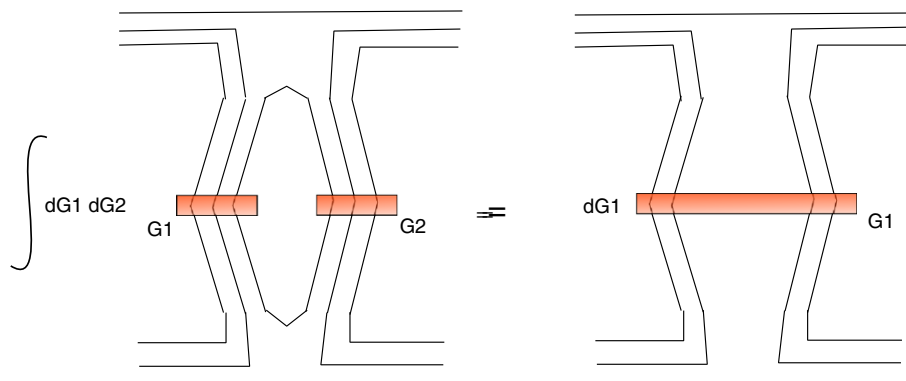


Figure 5 The integration rule for 2-dipoles.

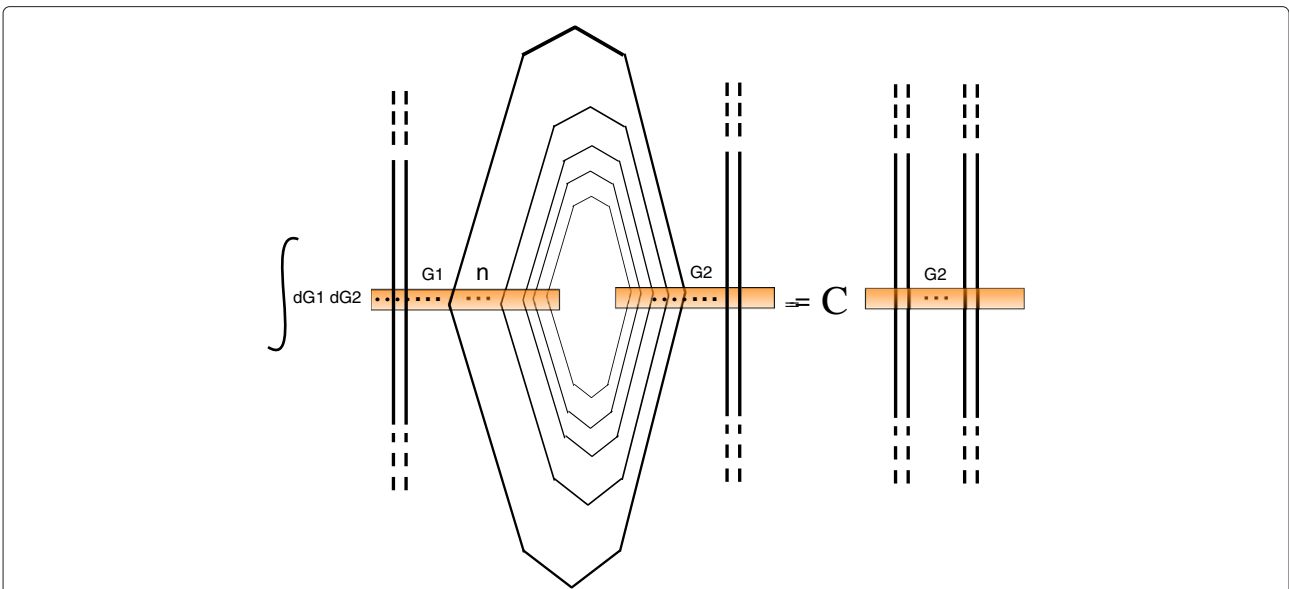


Figure 6 The integration rule for the reduction of concentric strands. The constant C is infinite and, regularized, is $[\delta^\Lambda(e)]^{n-1}$.

where Λ is the cutoff and K is a constant. For $D = 3$, this bound reduces to

$$A(G) \leq K^{2n} \Lambda^{3n/2+6}. \quad (8)$$

In particular, it is easy to prove that the following upper and lower bounds are valid for the sphere:

$$c_1 \Lambda^6 \leq \frac{A_{2n}(S^3)}{\lambda^n \bar{\lambda}^n} \leq c_2 \Lambda^{3(n+2)}. \quad (9)$$

In a certain sense, these bounds are trivial because the lower bound is (8) with no vertices and the upper bound is exactly the upper bound for a generic graph. These bounds are less trivial, however, because for the 3-sphere, these are saturated by the two graphs in Figure 4, the upper by the graph above, and the lower by the graph below. Here, however, we want to stress that it is this peculiar feature of divergencies itself which make the analysis of graphs associated with manifolds of higher dimension much more complicated. For this reason, in what follows, we will put forward a procedure in order to factorize diverging terms due to the sphere. We now introduce few identities which will be useful later. These are in Figures 8 and 9.

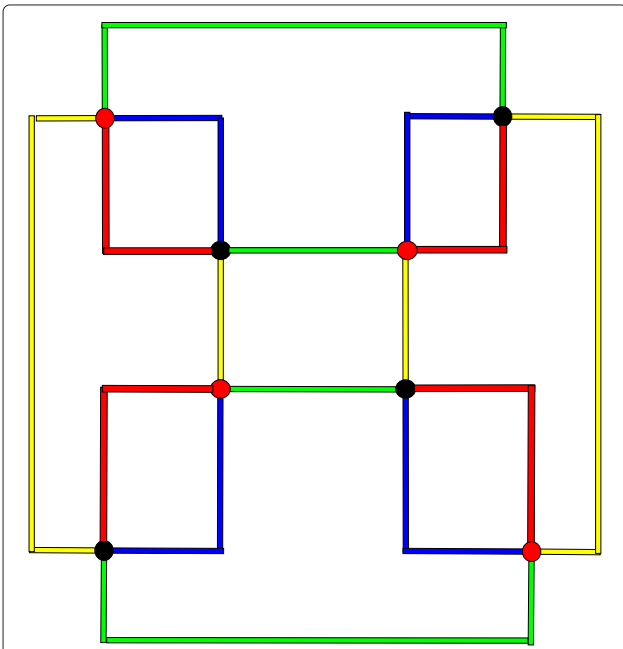


Figure 7 The minimal graph of the solid torus $S^1 \otimes S^2$.

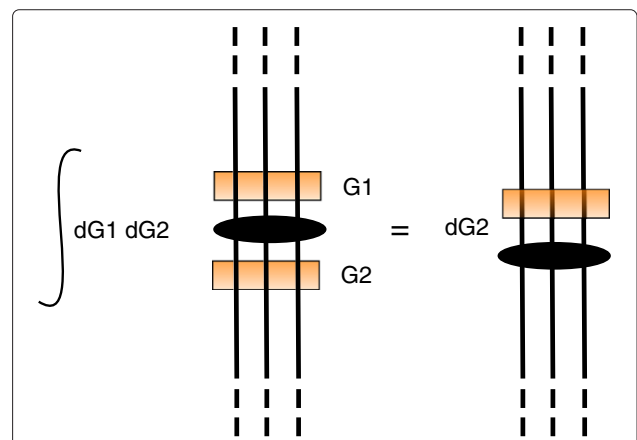


Figure 8 A graphical representation of the identity in Equation 10.

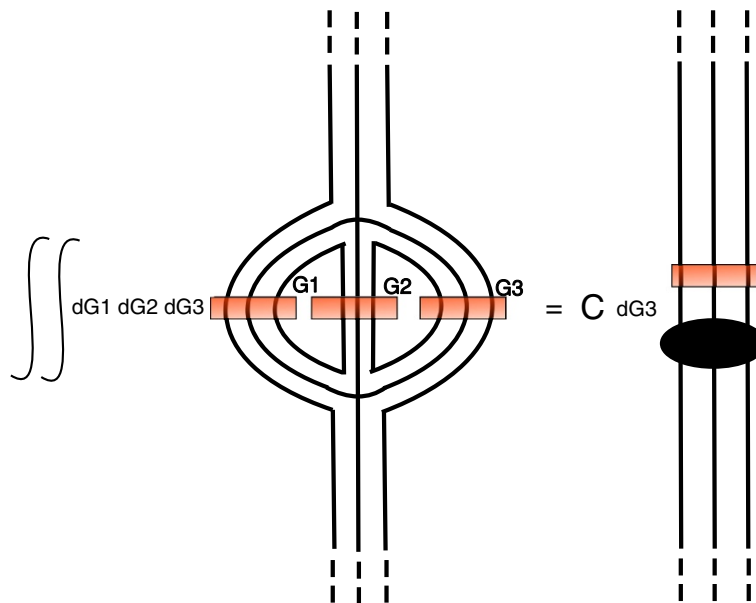


Figure 9 The integration rule for the contraction of a 3-dipole. The constant C is infinite and, regularized, is $\delta^\Lambda(e)$.

We first notice two identities. The first is the one in Figure 8, which comes from the following identity:

$$\int \int dg_1 dg_2 \delta(A_1 g_1 g_2^{-1} B_1) \delta(A_2 g_1 g_2^{-1} B_2) \delta(A_3 g_1 g_2^{-1} B_3) = \int dg_1 \delta(A_1 g_1 B_1) \delta(A_2 g_1 B_2) \delta(A_3 g_1 B_3) \quad (10)$$

Cuts, bounds, and spheres

Before going into the body of the paper, let us recall the technique of the cuts studied in [32]. For simplicity, we discuss colored vacuum graphs, but some of the arguments can be generalized to noncolored graphs with open lines. Let us consider here vacuum graphs of a GFT in D dimension over the group G . Consider two graphs, A and B , which are connected by a series of propagators

p_1, \dots, p_n with group elements $g_1, \dots, g_n \in G$. The total amplitude can be written as

$$A = \int \prod_i dg_i A(g_1, \dots, g_n) B^*(g_1, \dots, g_n) \quad (11)$$

where dg_i represents the Haar measure over the group. Since the functions A, B are real, it is easy to see that (11) has all the properties of a distance and so can be considered as a scalar product between the functions A and B , (A, B) . Since (11) is a scalar product, then it is bounded by the Cauchy-Schwarz inequality

$$(A, B)^2 \leq (A, A) (B, B).$$

We will call *cut* over the propagators p_1, \dots, p_n the bound given by the Cauchy-Schwarz inequality referred to the two parts of the graph, A and B , as depicted in Figure 10 for the colored model. In the colored Boulatov model, the complex structure requires the change of the

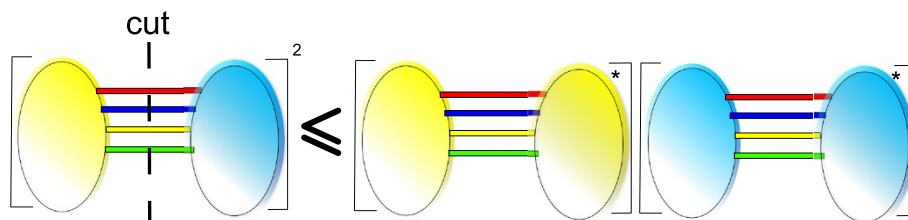
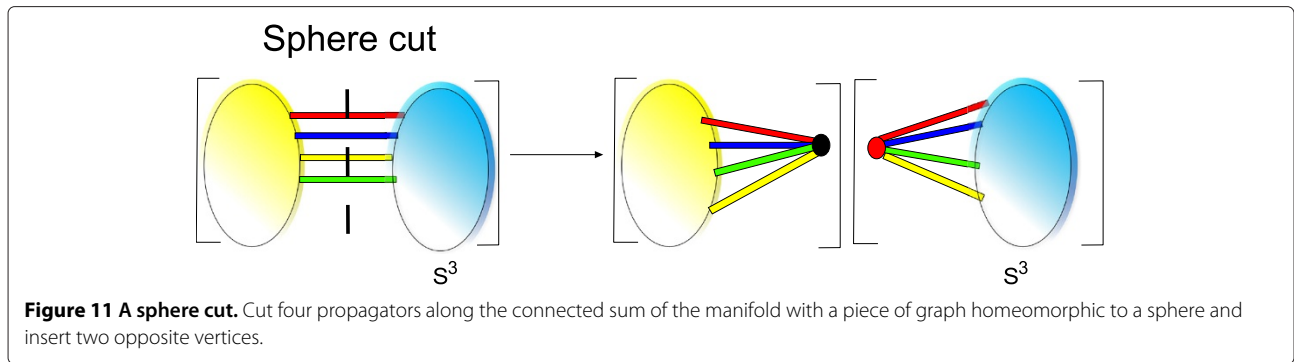


Figure 10 Cut rule for amplitudes. The cut can be done over all possible propagators. Here we focus on the case in which it cuts off only pieces of graphs homeomorphic to the sphere.



orientation of every vertex that is changing the color of the vertex (black \leftrightarrow red). The complex amplitude is then glued with its conjugate, as the star represents in Figure 10.

Let us now discuss the sphere decomposition of graphs and what we will call *sphere cuts*. Consider a graph generated by the colored Boulatov model which can be decomposed as in Figure 11, where two parts of the graphs are connected by a propagator. We call *topological cut* an insertion of two disconnected vertices with different orientations in the propagator where a manifold is connected to the boundary of a 3-ball. Since the amplitudes are invariant under color conjugation, we can always redefine the amplitude in such a way that the insertion is as in Figure 11. We say that we are cutting a sphere if one of the graphs can be reduced through nondegenerate fusion/contractions of 1- and/or 2-dipoles to a 3-ball (a vertex). This can be extended to more general graphs, where we decompose the graph into multi-spheres and consider their cuts. In order to see the result of our topological cuts on a concrete example, we apply this to the case of the connected sum of solid torii. The reason why we introduce this is that the solid torus is an easier example due to its structure and the structure of its core graph.

Solid torus decomposition

Consider now the graph in Figure 7 for the solid torus [33,34]. For a finite number of vertices, we can build the following decomposition by means of a connected sum of solid tori $T_3 = S^1 \otimes S^2$:

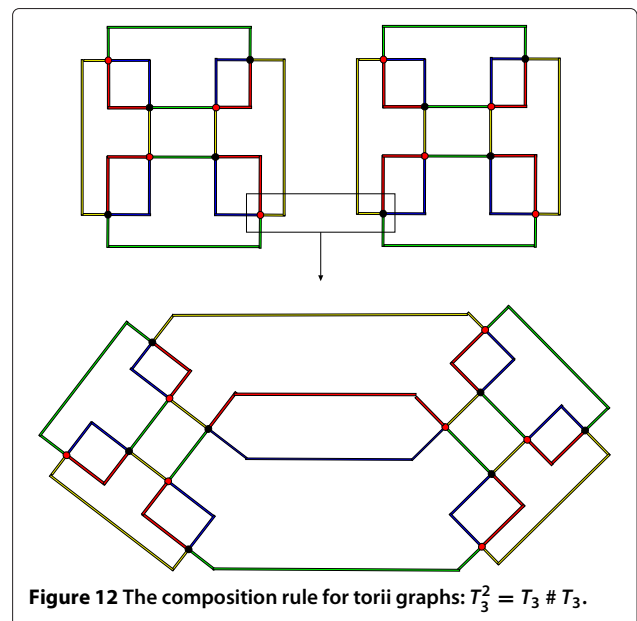
$$T_3^h = \underbrace{T_3 \# T_3 \# \dots \# T_3}_{h\text{-times}} \quad (12)$$

We now show that the divergence of this manifold with h – handles is related to the number of handles.

Lemma 1. *The divergence of the connected sum in (12) is for $h \geq 1$:*

$$\mathcal{A} \sim \lambda^{1+3h} \bar{\lambda}^{1+3h} [\delta^\Lambda(e)]^{2(h+1)}. \quad (13)$$

Proof. Consider the graph in Figure 7. This graph represents a solid torus built with the minimal number of vertices. By the theorem on the contraction of dipoles introduced antecedently, we can then construct the connected sum of solid 3-tori by joining two graphs as in Figure 12. In order to prove this fact, consider the diagram in Figure 13, and then the generic connected sum is an easier generalization of this one. In the top diagram of Figure 13, consider the 2-bubbles labeled with numbers from 1 to 7. Using the integration rule for 2-dipoles as in Figure 8, the diagram can be transformed with fewer integration over propagators, as in the second step of Figure 13. We now notice that there are concentric strands for each of the part of the diagram labeled by capital latin letters, labeled from A to E. Extract the divergence and put it aside using the integration rule for the reduction of concentric strands, as in Figure 6. For each latin letter, there is one power because there are two concentric strands. Having extracted the divergence, it is easy to notice that what is left is a ribbon graph generated by a two-dimensional GFT. Pick a maximal tree as in the green shadowed line as



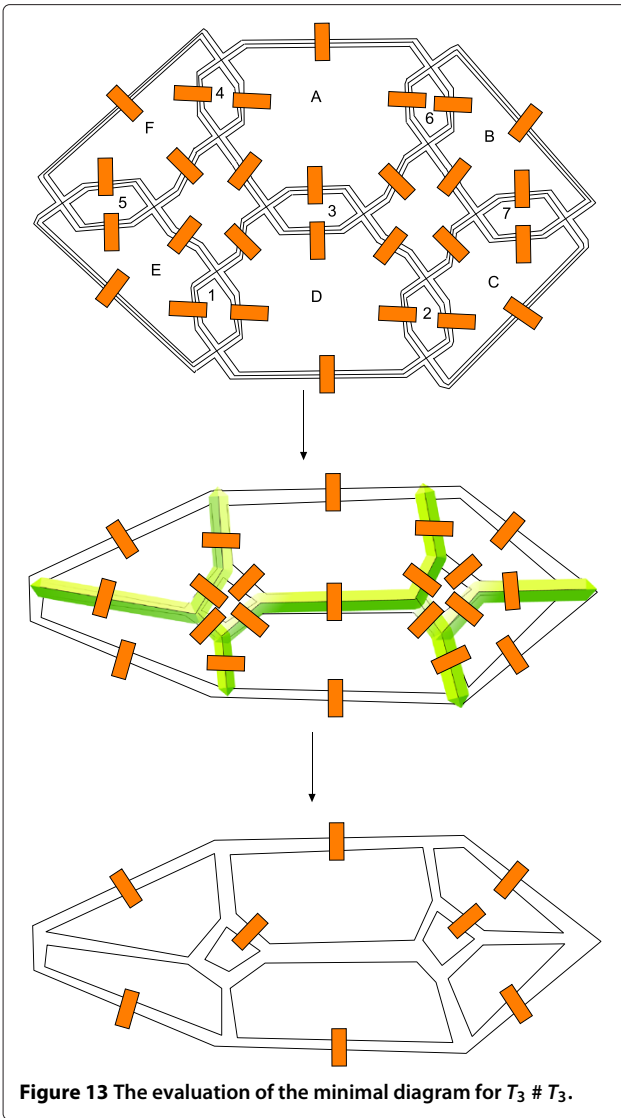


Figure 13 The evaluation of the minimal diagram for $T_3 \# T_3$.

in the second step of Figure 13 and set the propagators to one. What is left is a diagram as in step 3 of Figure 13. It is easy to see that this diagram is finite. All the steps, also the use of the maximal tree, can be generalized to several connected sums. It is then also easy to see, at this point, that the number of divergencies is related to the parts of the graph labeled with latin letters, and that can be counted

easily for generic connected sums. From here, it follows Equation 13. \square

Evaluating the bounds

We can now make a bound on generic genus- h manifolds as follows. We first recall the following norm as a cut over the propagators of a Feynman graph. Consider a graph split into two graphs by a series of cuts, as in Figure 10. Then the amplitude square is bounded by the norms of the left and right graphs contracted with themselves by converting a red vertex to a black vertex and vice versa. We can now use this trick in a clever way. It is well known in topology that every manifold is homotopic to itself modulo cutting off S^3 . We can then think of any manifold in a simplicial setting in which this manifold is constructed by $2k$ vertices, as a *minimal* one, made of $2j$ vertices then a connected sum of 3-spheres by a connected sum as explained in this section and leaving $2j - 2k$ vertices to this part. In the simplest case in which the simplicial complex is a minimal one and the connected sum of a sphere, we can consider the cut along the two vertices which make the connected sum, as in Figure 14. We now evaluate a bound on the divergence of graph representing T_r^h using Figure 10. It is well known in topology that every manifold is homotopic to itself modulo cutting off S^3 (Figure 15).

Following our the previous discussion, the bounds come from taking cuts [32] over edges on the connected sum of the minimal torus.

$$A_{2k}^2(T_3) \leq A_{14}(T^3 \# T^3) A_{2(k-7)}(S^3) \tag{14}$$

where, however, the divergence of the graph of $T^3 \# T^3$ is now minimal and has been evaluated in (13) for generic genus. Thus, the bound is on the divergence of the sphere, for which we can use the bounds introduced before. This kind of *homeomorphic* bounds can be generalized to other types of homeomorphic manifolds as, for instance, connected sums of torii, as we will do later in the paper. In this case, the bound takes the following form:

$$A_{2k}^2(\underbrace{T_3 \# T_3 \# \dots \# T_3}_{n\text{-times}}) \leq \leq A_{6n+2}(\underbrace{T_3 \# T_3 \# \dots \# T_3}_{2n\text{-times}}) A_{2k-6n-2}(S^3) \tag{15}$$

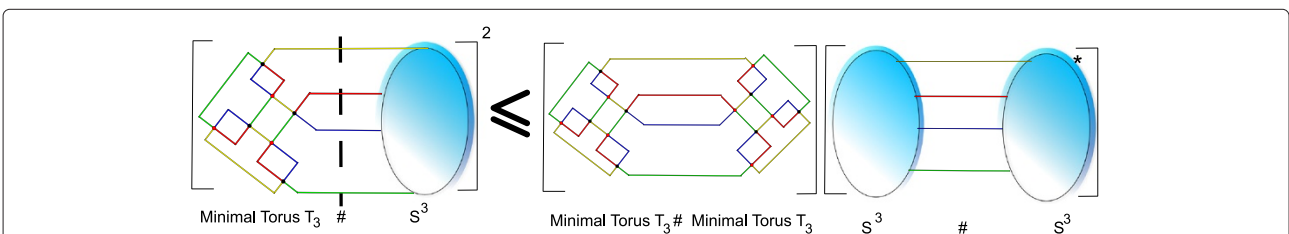
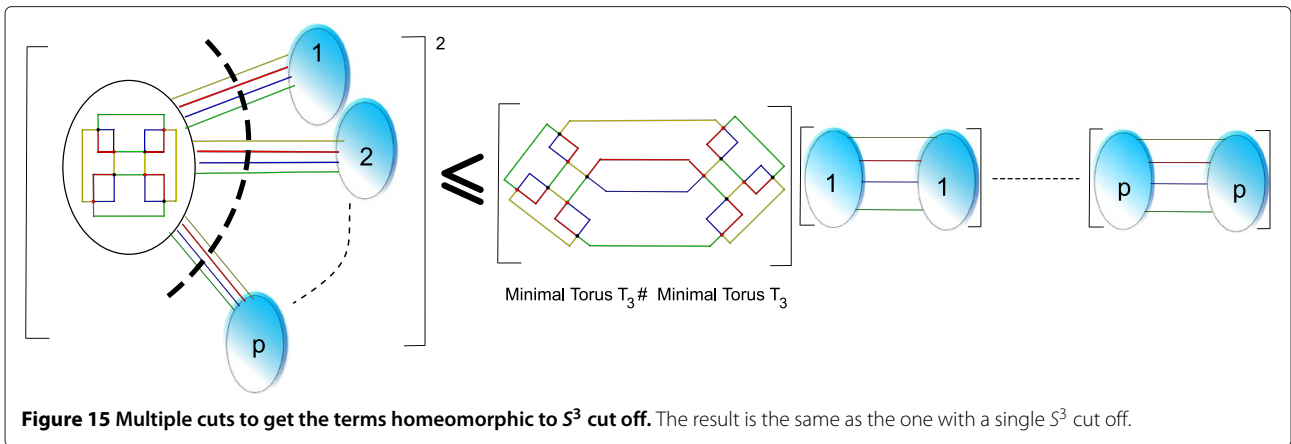
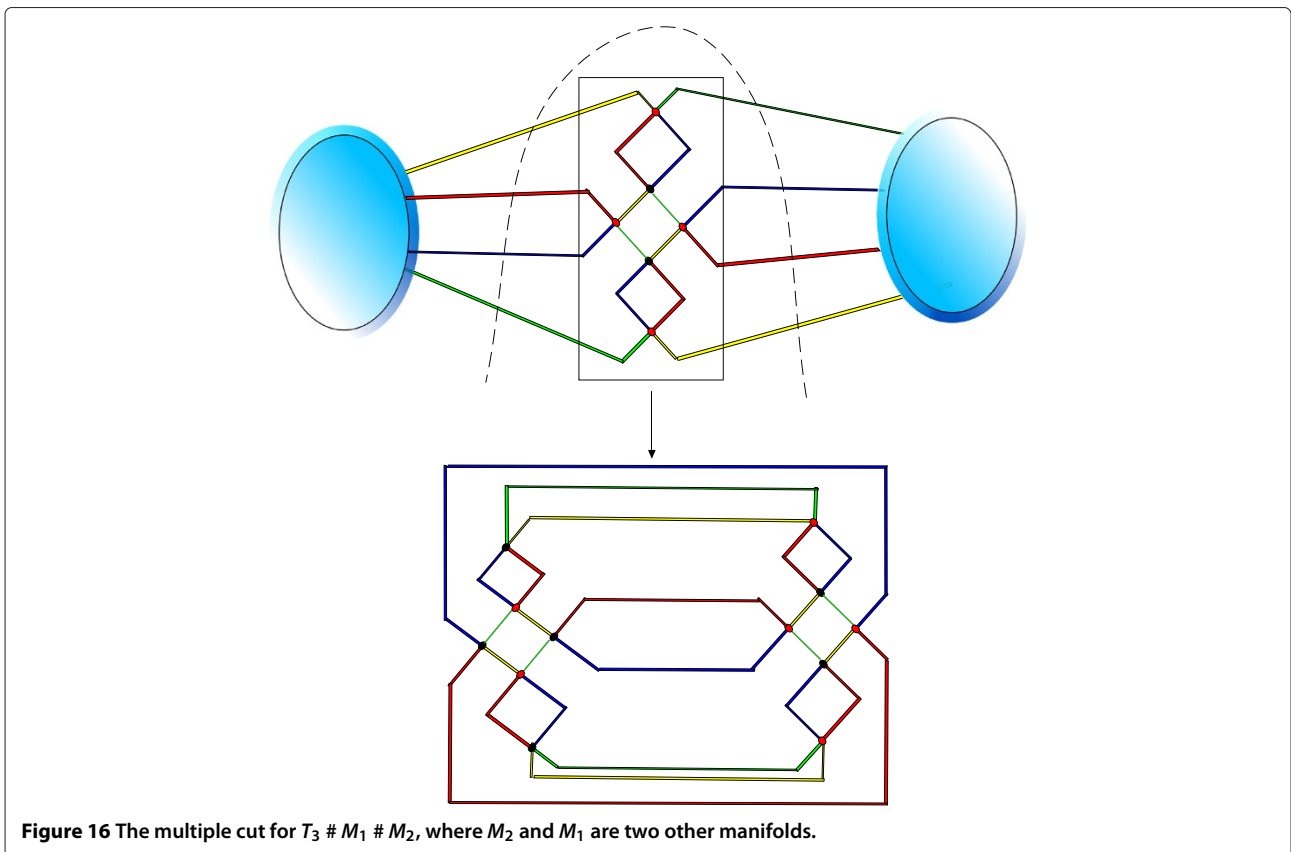


Figure 14 The cut applied on the connected sum of a minimal torus and a sphere. This procedure put the uncertainty of the divergence of the graph on the graph of the sphere, which is easier to study.



where you cut only one sphere. In this case, each connected sum of torii with h handles is bounded by a canonical $2h$ handle, which is evaluated in general, and multiple amplitudes on the spheres, depending on whether there are one or more cuts, as in Figure 14. This identity is related to the well-known fact $\mathcal{M} \simeq \mathcal{M} \# S^3$. This formula shows that the ‘uncertainty’ of the divergencies of a generic triangulation of a 3-manifold can be split into a canonical decomposition, thanks to the theorem on the contraction of 1-dipoles, and put in relation with solid

tori, and put the uncertainty into a different graph homeomorphic to the spheres. There is, however, a subtlety due to the fact that in general a manifold can be seen as many connected sums of the same manifold with spheres. In this case, a feasible cut should be on multiple propagators connecting spheres, as in Figure 16. However, it is easy to understand that each time you make a *single* cut between an h -handle diagram and a sphere, the diagram for the handle part is a connected sum of the same two h -handles and thus becomes a $2h$ handle diagram. However,



when there are multiple cuts, the same diagram is connected multiple times with itself. It is easy to understand that making a unique cut along all the pieces homeomorphic to the spheres can glue the torii with themselves more than once, making them noncanonical, and thus making it difficult to recognize the handle decomposition. In principle, this should be performed one cut at a time. However, performing one cut at a time doubles the number of pieces homeomorphic to the sphere. A possible trick would be to make this an infinite number of times:

$$\begin{aligned} & \mathcal{A}^2(\underbrace{T_3 \# \dots \# T_3}_{k\text{-times}} \# \underbrace{S_3 \# \dots \# S_3}_{p\text{-vertices}}) \leq \\ & \leq \lim_{n \rightarrow \infty} \{ \mathcal{A}(\underbrace{T_3 \# \dots \# T_3}_{2nk\text{-times}} \# \underbrace{S_3 \# \dots \# S_3}_{\text{the rest}}) \}^{\frac{1}{n}} \cdot \\ & \cdot \sqrt{A_{i_n}(S_3)} \sqrt{\dots \sqrt{A_{i_2}(S_3)} \sqrt{A_{i_1}(S_3)} A_{i_0}(S_3)} \end{aligned} \quad (16)$$

Now you would expect that in the $n \rightarrow \infty$ limit,

$$\mathcal{A}(\underbrace{T_3 \# \dots \# T_3}_{2nk\text{-times}} \# \underbrace{S_3 \# \dots \# S_3}_{\text{the rest}})$$

becomes a canonical connected sum of torii, which we know how to evaluate. However, a careful thought will show that this cannot happen. The reason is that while the number of cuts increases linearly, the number of spheres increases as 2^n . Thus, in order to extract the divergencies due to the sphere in the bound, neat sequences of cuts have to be made. In the following, we will, for simplicity, represent a propagator as a solid line and cuts as bold dashed lines, as in Figure 17.

As we have shown before, an infinite number of cut limit is not feasible. Thus, we have to choose the sequence of cuts in a clever way. In particular, note that when you perform a cut, the number of spheres doubles. The trick is to double also the number of spheres cut at each step. For instance as in Figure 17, the first cut is on one sphere, the second cut is on the two S_2 spheres, the third on the four S_3 spheres, and so on. In this way, the number of cuts is n before we exhaust the number of spheres. Each n th cut separates 2^n spheres. Carrying all the cuts until the end gives the following bound:

$$A(G \# S_1^3 \# \dots \# S_n^3) \leq (A(Q^n))^{\frac{1}{2^n}} \prod_{i=1}^n \sqrt{A(S_i \# S_i)} \quad (17)$$

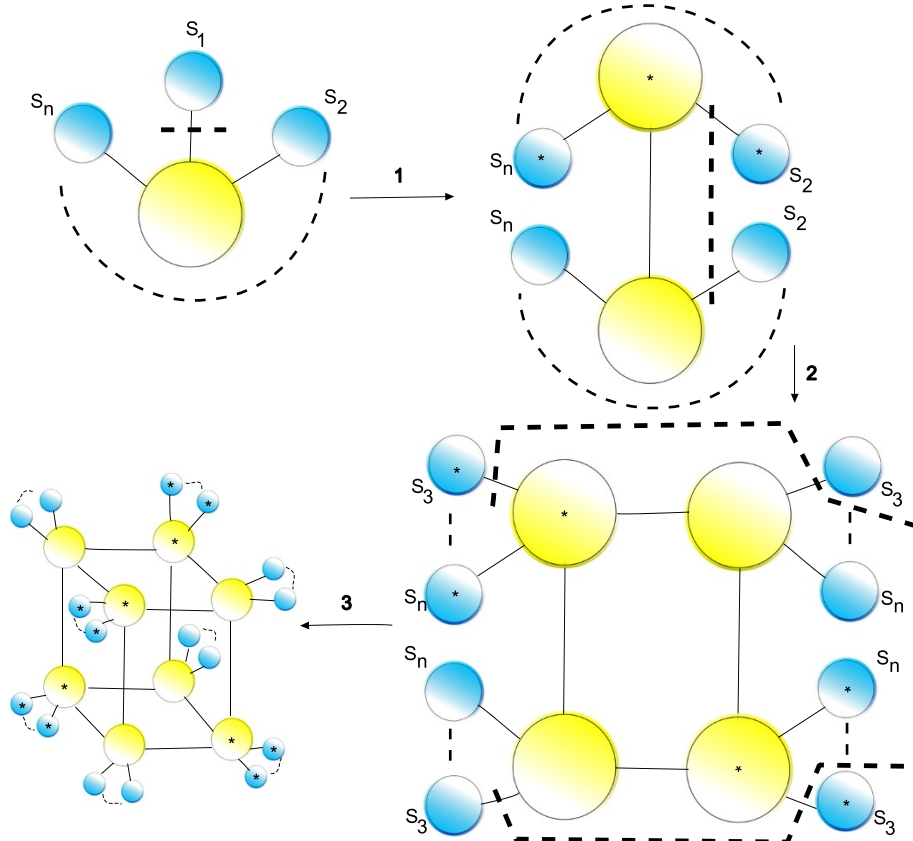


Figure 17 The first three cuts of the sequence for a connected sum with n different spheres, S_j .

Now Q^n is a very particular graph which depends on the number of spheres but has a typical form for $n > 2$, and which we now explain. The case $n = 1$ is special. To give a graphical representation, if the amplitude was a single vertex, the resulting amplitude at the $(n-1)th$ cut would be a piece of $(n-1)$ -dimensional cubic lattice where at each point the S_n sphere is attached. The case $n = 1$ is trivial. In Figure 18, the graphs are generated by the sequence of cuts in the cases $n = 1, \dots, 4$. Notice that these cuts are well behaved from the topological point of view. In fact, when we do a cut on a sphere, for instance in the $n = 1$ case, what we are doing is the following: take a manifold and remove a ball B^3 from it, then take the same manifold, reverse the orientation, carve a ball B^3 , and identify the boundaries between the two. This is the same as ordinary surgery in topology. Let us define now the following surgery operation $\#^n$: carve n balls out of a manifold, copy the manifold with an opposite orientation, and identify the boundary of these balls pairwise. We now have all the elements to give a proper definition for the quantity Q^n . Let \mathcal{G} be the topological manifold associated with G . Then the resulting Q^n manifold is constructed by recursively cutting and pasting as follows:

$$\begin{aligned} Q^1 &= \mathcal{G} \# \mathcal{G} \\ Q^2 &= (\mathcal{G} \# \mathcal{G}) \#^2 (\mathcal{G} \# \mathcal{G}) \end{aligned} \quad (18)$$

In general, this is defined for a generic n as

$$Q^n = Q^{n-1} \#^n Q^{n-1}. \quad (19)$$

Thus, Equation 17 gives a compact bound, trivializing the contribution of the spheres if these are strategically separated by means of cuts. For the case of solid torii, in particular, the divergence can be evaluated and related to the number of handles, which behave nicely under the surgery explained. In principle, this bound, given the smallest representation of a topological manifold in terms of simplices, can be explicitly evaluated. On the other hand, the evaluation of the graph Q^n can be quite cumbersome. Another possible cut, which is quite economical, is given by the single cut of all the spheres together. This cut, once performed, leaves us with what we will call a 'core graph' (Figure 19). For this cut, the $n = 8$ case is the simplest way to evaluate for the solid torus, while it is $n = \nu_{\text{vert}}$ case for a generic graph with ν_{vert} vertices. Using the integration rule for concentric strands, the resulting graph becomes counting the number of circles in the graph (Figure 20). In this case, in fact, there is a $\delta^\Lambda(e)^2$ because a propagator is made of three internal strands. For the solid torus, n can be as big as 8, which would be the most general case to evaluate. To give an example of how to evaluate this bound, we evaluate the cases $n = 1, \dots, 4$

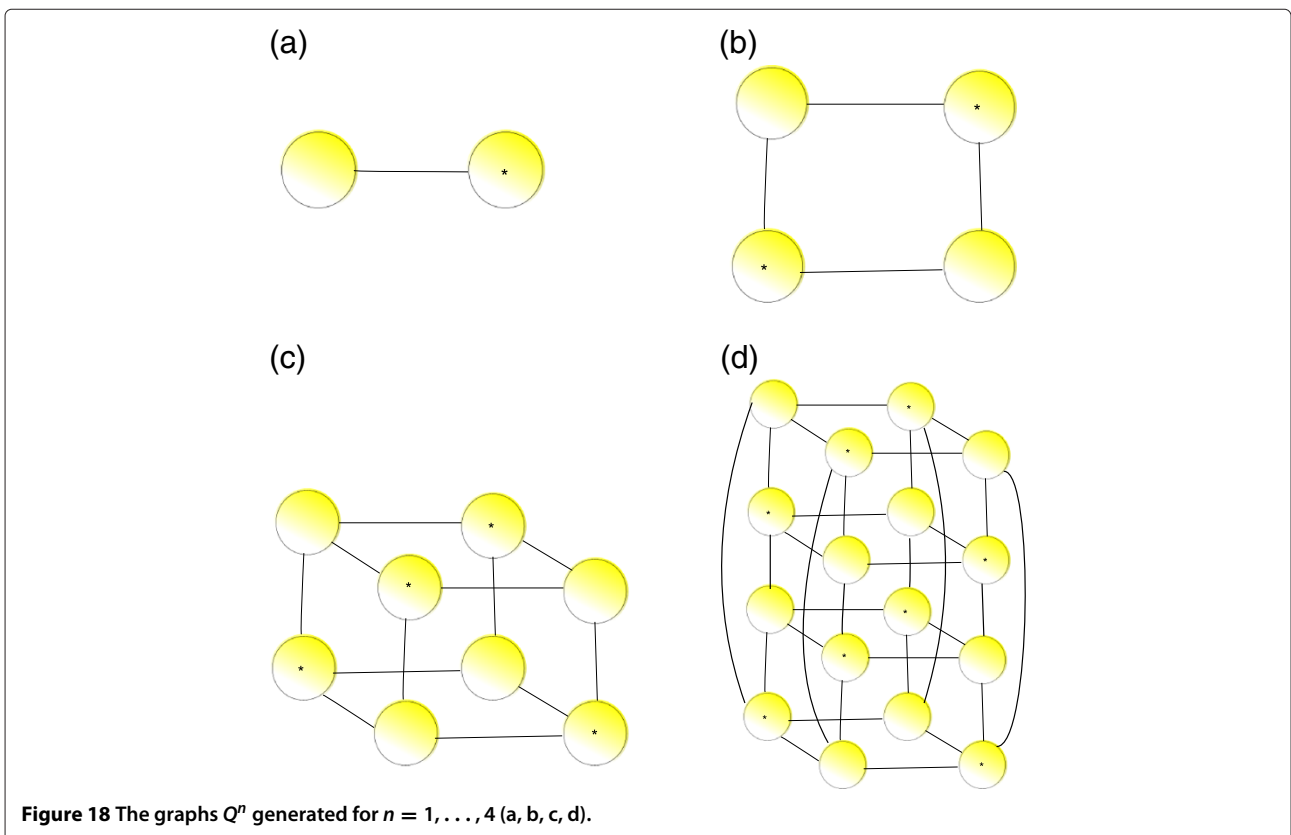
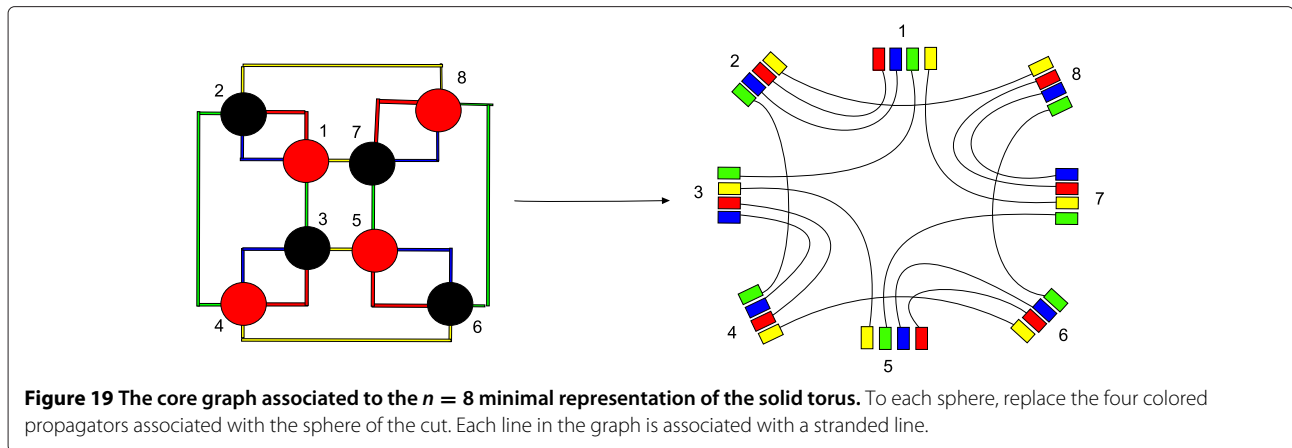


Figure 18 The graphs Q^n generated for $n = 1, \dots, 4$ (a, b, c, d).



for the solid torus, showing how it works for $n = 2$ and giving the final results for $n = 3, 4$.

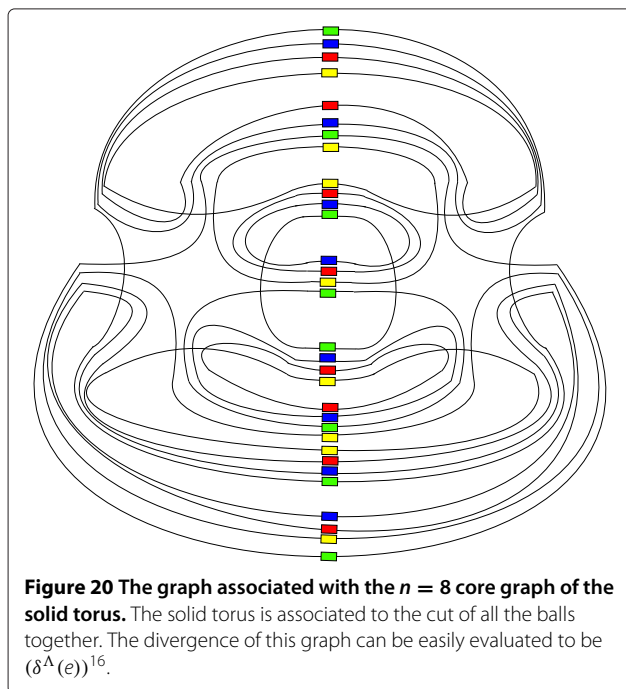
A naïve large N limit for solid torii

We now have the possibility, using this exact result for canonical graphs and the motivated conjecture on the maximum divergence of the sphere, to perform a 't Hooft limit in the couplings. Let us consider now the renormalized couplings:

$$\lambda \rightarrow \frac{\lambda_0}{\delta^\Lambda(e)}; \quad \bar{\lambda} \rightarrow \frac{\bar{\lambda}_0}{\delta^\Lambda(e)}.$$

Using the upper bound, we can see that as

$$\sup A_{2k}(S^3) \sim [\delta^\Lambda(e)]^{1-n}$$



and

$$A_{2k}(T_3^h) \sim [\delta^\Lambda(e)]^{-4h}.$$

It is easy to see that the first order of the sphere does not diverge, while the higher the number of handles, the higher the graph is suppressed in the weak coupling limit. This is compatible with the result obtained in [16].

It is, however, easy to understand that these are valid for *minimal* graphs for solid torii. Let us then use the bound given by (15) given by cutting only one sphere of $2n$ vertices. In this case,

$$\sup A_{2k}(T_3^h) \sim [\delta^\Lambda(e)]^{-4h+n+1}.$$

Thus, there is a competition between the number of handles of the canonical graph and the vertices associated to the sphere which has been cut.

Conclusion

Group field theories provide one of the most promising framework for a background-free theory of quantum gravity in which one sums both over topologies and geometries. The important feature of the model rests on the structure of the divergencies, related to the structure of the Feynman graphs. It has been shown, under a proper regularization of the integrals preserving the group structure underlying the theory, that graphs topologically equivalent to sphere dominate the partition function when the only cutoff is sent to infinity in the renormalized couplings. If the coupling is kept finite, however, other topologies contribute to the partition function, and indeed it has been shown that they are combinatorially favored in the expansion to the spherical topology. In this paper, we focused on the topology related to the dual of the Feynman graphs in the perturbative expansion of the partition function and introduced a formalism of cuts in order to separate divergencies related to different topologies. We believe this to be a novel technique aimed at

analyzing and factorizing the contribution to the divergence degree due to the sphere. These techniques relied heavily on the graph coloring, thus valid only in a colored group field theory, and are aimed at constructing amplitude bounds using propagator cuts. We showed that cutting along propagators, the dual can be interpreted as points in which a connected sum of two manifolds is performed and can factorize the divergencies of the two topologies. In particular, if the cut is performed where a sphere is connected, then a specific bound can be taken as spheres are very well studied in group field theory. Color is a fundamental ingredient in this paper as the connected sum can be defined only on the base of dipole contractions. After having introduced the technique, we applied it to the connected sum of solid torii as an example.

Although several powerful and precise results on the divergence of generic Feynman diagrams already exist [14], in relation to both the group and the structure of the graph Γ , it is clear that the divergences of a Feynman diagram are not related only to the topology of the bubbles but are indeed intertwined with the topology of the dual of the graph Γ . In this respect, we believe that the formalism introduced in the present paper could contribute to the understanding of the contributions related to the topology of dual graphs in Group Field Theory. The sphere cuts can be introduced in order to introduce topological surgery into the matter of calculating divergence bounds on a particular graphs.

The limitation of such approach is its lack of generality in providing a sequence of cuts for generic topologies. The sphere cut formalism might be useful in the study of graphs of specific topology. It has been for long stressed that the partition function of a quantum gravitational theory has to have a sum over all the possible topology. Our approach might be helpful in understanding the different behavior, in terms of divergencies, of two topologies connected by a topological surgery operation.

Competing interests

The author declares that he has no competing interests.

Acknowledgements

We would like to thank Daniele Oriti, Sylvain Carrozza, Joseph Ben-Geloun, Lorenzo Sindoni, and Dan Lynch for several discussions. Moreover, we would like to thank the anonymous referees for the valuable comments. This research has been mostly conducted while visiting the Albert Einstein Institute (MPI) in Berlin, where financial support has also been given.

Received: 22 May 2013 Accepted: 3 November 2013

Published: 21 November 2013

References

1. Oriti, D: The microscopic dynamics of quantum space as a colored group field theory. In: Ellis, G, Murugan, AWJ (eds) *Foundations of Space and Time: Reflections on Quantum Gravity*. Cambridge University Press, Cambridge (2011)
2. Gurau, R, Ryan, JP: Colored tensor models - a review. *SIGMA* **8** (2012). doi:10.3842/SIGMA.2012.020

3. Oriti, D: The group field theory approach to quantum gravity: some recent results. In: Kowalski-Glikman, J, Kowalski-Glikman, J, Durka, R, Szczachor, M (eds.) *THE PLANCK SCALE: Proceedings of the XXV Max Born Symposium*. AIP: conference proceedings. AIP, Melville (2009)
4. Perez, A: The spin foam approach to quantum gravity. *Living Rev. Relativity* **16**, 3 (2013)
5. Brezin, E, Itzykson, C, Parisi, G, Zuber, JB: Planar diagrams. *Commun. Math. Phys.* **59**, 35 (1978)
6. David, F: A model of random surfaces with nontrivial critical behavior. *Nucl. Phys. B* **257**, 543 (1986)
7. Gurau, R: Lost in translation: topological singularities in group field theory. *Class. Quant. Grav.* **27**, 235023 (2010)
8. Gurau, R: Colored group field theory. *Commun. Math. Phys.* **304**, 69 (2011)
9. Oriti, D: The quantum geometry of tensorial group field theories. In: *Proceedings of the XXIX International Colloquium on Group-Theoretical Methods in Physics, Tianjin. 20–26 August 2012*
10. Gurau, R: Universality for random tensors. arXiv:1111.0519 (2011)
11. Geloun, JB, Krajewski, T, Magnen, J, Rivasseau, V: Linearized group field theory and power counting theorems. *Class. Quant. Grav.* **27**, 155012 (2010)
12. Freidel, L, Gurau, R, Oriti, D: Group field theory renormalization - the 3d case: power counting of divergences. *Phys. Rev. D* **80**, 044007 (2009)
13. Magnen, J, Noui, K, Rivasseau, V, Smerlak, M: Scaling behaviour of three-dimensional group field theory. *Class. Quant. Grav.* **26**, 185012 (2009)
14. Bonzom, V, Smerlak, M: Bubble divergences from cellular cohomology. *Lett. Math. Phys.* **93**, 295 (2010)
15. Carrozza, S, Oriti, D, Rivasseau, V: Renormalization of an SU(2) tensorial group field theory in three dimensions. arXiv:1303.6772 (2013)
16. Gurau, R: The $1/N$ expansion of colored tensor models. *Ann. Henri Poincaré* **12**, 829–847 (2010)
17. Pezzana, M: Sulla struttura topologica delle varietà compatte. *Atti Sem. Mat. Fis. Univ. Modena* **23**, 269–277 (1974)
18. Lins, S: *Gems, Computers and Attractors for 3-Manifolds; Series on Knots and Everything*, vol 5. World Scientific, Singapore (1995)
19. Caravelli, F: A simple proof of orientability in the colored Boulatov model. *SpringerPlus* **1**, 6 (2012)
20. Gurau, R: The complete $1/N$ expansion of colored tensor models in arbitrary dimension. *Ann. Henri Poincaré* **13**, 399 (2012)
21. Bonzom, V, Gurau, R, Riello, A, Rivasseau, V: Critical behavior of colored tensor models in the large N limit. *Nucl. Phys.* **B853**, 174–195 (2011)
22. Carrozza, S, Oriti, D: Bubbles and jackets: new scaling bounds in topological group field theories. *HEP* **2012**(6), 92 (2012)
23. Carrozza, S, Oriti, D, Rivasseau, V: Renormalization of tensorial group field theories: Abelian U(1) models in four dimensions. arXiv:1207.6734 (2012)
24. Ryan, JP: Tensor models and embedded Riemann surfaces. *Phys. Rev. D* **85**, 024010 (2012)
25. Geloun, JB, Rivasseau, V: A renormalizable 4-dimensional tensor field theory. *Comm. Math. Phys.* **318**, 1 (2011)
26. Geloun, JB: Renormalizable models in rank $d \geq 2$ tensorial group field theory. arXiv:1306.1201 (2013)
27. Rivasseau, V: Spheres are rare. *Europhysics Letters* **102**, 61001 (2013)
28. Gurau, R: The $1/N$ expansion of tensor models beyond perturbation theory. arXiv:1304.2666 (2013)
29. Milnor, J: A unique decomposition theorem for 3-manifolds. *A. J. Math.* **84**, 1–7 (1962)
30. Boulatov, DV: A model of three-dimensional lattice gravity. *Mod. Phys. Lett. A* **7**, 1629 (1992)
31. Ferri, M, Gagliardi, C, Grasselli, L: Crystallisation moves. A graph-theoretical representation of PL-manifolds - a survey on crystallizations. *Aequationes mathematicae* **31**, 121 (1986)
32. Geloun, JB, Magnen, VRJ: Bosonic colored group field theory. *Eur. Phys. J.* **C70**, 1119–1130 (2010)
33. Gagliardi, C: Recognizing a 3-dimensional handle among 4-coloured graphs. *Ricerche Mat.* **31**, 389–404 (1982)
34. Lins, S: A simple proof of Gagliardi's handle recognition theorem. *Discrete Math.* **57**, 253–260 (1985)

doi:10.1186/2251-7235-7-63

Cite this article as: Caravelli: GEMs and amplitude bounds in the colored Boulatov model. *Journal of Theoretical and Applied Physics* 2013 **7**:63.